Transcription factor 7-like 1 is involved in hypothalamo–pituitary axis development in mice and humans

Carles Gaston-Massuet[a,1], Mark J. McCabe[b,2,3], Valeria Scagliotti[c], Rodrigo M. Young[d], Gabriela Carreno[a], Louise C. Gregory[b], Sujatha A. Jayakody[a], Sara Pozzi[a], Angelica Gualtieri[c], Basudha Basu[e], Markela Koniordou[a], Chun-I Wu[f], Rodrigo E. Bancalari[b], Elisa Rahikkala[g,h], Riitta Veijola[i], Tuija Lopponen[j], Federica Graziola[c], James Turton[b], Massimo Signore[a], Seyedeh Neda Mousavy Gharavy[a], Nicoletta Charolidi[a], Sergei Y. Sokol[e], Cynthia Lilian Andoniadou[a,4], Stephen W. Wilson[d], Bradley J. Merrill[f], Mehul T. Dattani[b,5], and Juan Pedro Martinez-Barbera[a,5,6]

[a]Birth Defects Research Centre, Developmental Biology and Cancer Programme, University College London Institute of Child Health, London, WC1N 1EH, United Kingdom; [b]Genetics and Epigenetics in Health and Disease Section, Genetics and Genomic Medicine Programme, University College London Institute of Child Health, London WC1N 1EH, United Kingdom; [c]Centre for Endocrinology, William Harvey Research Institute, Barts and the London School of Medicine and Dentistry, Queen Mary University of London, London EC1M 6BQ, United Kingdom; [d]Department of Cell and Developmental Biology, University College London, London WC1E 6BT, United Kingdom; [e]Developmental and Regenerative Biology, Mount Sinai School of Medicine, New York, NY 10029; [f]Department of Biochemistry and Molecular Genetics, University of Illinois, Chicago, Illinois, IL 60607; [g]Research Unit for Pediatrics, Dermatology, Clinical Genetics, Obstetrics and Gynecology (PEDEGO) and Medical Research Center (MRC) Oulu, University of Oulu, FIN-90029, Oulu, Finland; [h]Department of Clinical Genetics, Oulu University Hospital, FIN-90029, Oulu, Finland; [i]Department of Pediatrics, PEDEGO and MRC Oulu, Oulu University Hospital, University of Oulu, FIN-90014, Oulu, Finland; and [j]Department of Child Neurology, Kuopio University Hospital, FIN 70029, Kuopio, Finland

Aberrant embryonic development of the hypothalamus and/or pituitary gland in humans results in congenital hypopituitarism (CH). Transcription factor 7-like 1 (TCF7L1), an important regulator of the WNT/β-catenin signaling pathway, is expressed in the developing forebrain and pituitary gland, but its role during hypothalamo–pituitary (HP) axis formation or involvement in human CH remains elusive. Using a conditional genetic approach in the mouse, we first demonstrate that TCF7L1 is required in the prospective hypothalamus to maintain normal expression of the hypothalamic signals involved in the induction and subsequent expansion of Rathke's pouch progenitors. Next, we reveal that the function of TCF7L1 during HP axis development depends exclusively on the repressing activity of TCF7L1 and does not require its interaction with β-catenin. Finally, we report the identification of two independent missense variants in human TCF7L1, p.R92P and p.R400Q, in a cohort of patients with forebrain and/or pituitary defects. We demonstrate that these variants exhibit reduced repressing activity in vitro and in vivo relative to wild-type TCF7L1. Together, our data provide support for a conserved molecular function of TCF7L1 as a transcriptional repressor during HP axis development in mammals and identify variants in this transcription factor that are likely to contribute to the etiology of CH.

WNT pathway | pituitary | Tcf7l1 | septooptic dysplasia | hypopituitarism

Congenital hypopituitarism (CH) is a complex condition defined by the deficiency of one or more pituitary hormones and can be present in isolation or as part of a syndrome (1–3). Septooptic dysplasia (SOD) is a rare form of CH (1 in 10,000) that manifests in conjunction with defects in the telencephalon (e.g., corpus callosum and septum pellucidum) and/or eyes (e.g., optic nerve hypoplasia) and is associated with high morbidity and occasional mortality (4).

Abnormal embryonic development of the hypothalamo–pituitary (HP) axis is a major cause of CH. The pituitary gland, comprising the anterior and posterior lobes, is an organ of dual embryonic origin, and derives from oral and neural ectoderm, respectively. In the mouse at around 9.5 d postcoitum (dpc), secreted signals from the hypothalamic primordium such as fibroblast growth factor (FGF) 8, FGF10, bone morphogenetic protein 4 (BMP4), and sonic hedgehog (SHH) induce Rathke's pouch (RP), the primordium of the anterior pituitary (5, 6). Upon specification, RP progenitors proliferate rapidly, exit the cell cycle, and activate

the expression of cell fate commitment genes such as POU domain, class 1, transcription factor 1 [*Pou1f1* (*Pit1*)], *Tpit*, and *Sf1*. This process culminates in the differentiation of all hormone-producing cells by the end of gestation (7, 8): somatotrophs [growth hormone

Significance

The relevance of transcription factor 7-like 1 (TCF7L1) during hypothalamo–pituitary (HP) axis development remains unknown. Using mouse genetics, we show that TCF7L1 acts as a transcriptional repressor to regulate the expression of the hypothalamic signals involved in pituitary formation. In addition, we screened a cohort of human patients with forebrain and/or pituitary defects and report two independent missense variants, p.R92P and p.R400Q, in human TCF7L1. Functional studies in vitro and rescue experiments in zebrafish mutants deficient for *tcf7l1a* and *tcf7l1b* show that the p.R92P and p.R400Q variants exhibit reduced repressing activity compared with wild-type TCF7L1. In summary, we identify TCF7L1 as a determinant for the establishment of HP axis development and as a potential candidate gene to be mutated in congenital hypopituitarism.

Table 1. Genotypes of offspring from Hesx1^Cre/+;TCF7L1^+/− x Tcf7l1^fl/fl genetic crosses

	Genotype,* n (% observed)				
Offspring	Hesx1^+/+;Tcf7l1^fl/+	Hesx1^+/+;Tcf7l1^fl/−	Hesx1^Cre/+;Tcf7l1^fl/+	Hesx1^Cre/+;Tcf7l1^fl/−	Total, n
Embryos[†]	21 (26.9)	19 (24.4)	17 (21.8)	21 (26.9)	78
Pups[‡]	9 (30.0)	10 (33.3)	6 (20.0)	5 (16.7)	30

*Twenty-five percent expected for each genotype; derived from expected Mendelian ratios.
[†]χ^2 test showed no significant deviation from the expected Mendelian ratio.
[‡]χ^2 test showed no significant deviation from the expected 25% ratio.

(GH)], lactotrophs [prolactin (PRL)], thyrotrophs [thyroid-stimulating hormone (TSH)], gonadotrophs [follicle-stimulating hormone (FSH) and luteinizing hormone (LH)], corticotrophs [adrenocorticotropic hormone (ACTH)], and melanotrophs [melanocyte-stimulating hormone (MSH)] (2, 9). A small proportion of cells remain in the postnatal anterior pituitary as tissue-specific stem cells, which have the capacity to self-propagate and differentiate in vivo and in vitro (10–12).

Mutations in several developmental genes regulating HP development in the mouse have been identified in patients suffering from CH and SOD (4). One of these is the homeobox gene *Hesx1/HESX1*, which acts as a transcriptional repressor of the WNT/β-catenin signaling pathway (13, 14).

The stability of β-catenin, which is a strong transcriptional activator devoid of a DNA binding domain, is critical for normal WNT/β-catenin function (15–17). In the absence of WNT ligands, β-catenin is phosphorylated by a destruction complex and degraded rendering the pathway inactive (18, 19). The binding of WNT ligands leads to β-catenin dephosphorylation and stabilization (20, 21). β-Catenin can then translocate into the nucleus and interact with mainly, but not exclusively, members of the T-cell factor/lymphoid enhancer factor (TCF/LEF) family to activate the expression of target genes (22, 23). In mammals, TCF/LEF factors include TCF7 (formerly TCF1), transcription factor 7-like 1 (TCF7L1) (formerly TCF3), TCF7L2 (formerly TCF4), and LEF1, which all bind the same consensus DNA motif 5′-(A/T)(A/T)CAAAG-3′ and have a β-catenin–interacting domain at the N terminus (24, 25). It is believed that, in the absence of stable β-catenin, TCF/LEF factors can repress target genes of the pathway through interactions with corepressors (26, 27), although cell context-specific functions have been demonstrated where specific factors are mostly required as either activators (28, 29) or repressors (30–33).

In the developing HP axis, this pathway coordinates proliferation of RP progenitors and differentiation of hormone-producing cells (34–41). TCF7L1 has been shown to play critical roles in maintenance of stem cell pluripotency (42, 43), tissue homeostasis of the skin epithelia (44), cell lineage determination during gastrulation (45, 46), and brain development in vertebrates (47, 48). However, the function of this important transcriptional factor during HP axis development has not been investigated to date. Moreover, despite the solid evidence demonstrating the critical function of the WNT/β-catenin pathway during HP axis development in the mouse, to date, mutations in components of this pathway have not been identified in patients with CH. In this study, we reveal that the β-catenin–independent repressor activity of TCF7L1 is required for normal HP axis formation in mice and humans.

Materials and Methods

Mice. The *Hesx1^Cre/+* (49), *Tcf7l1^flox/flox* (44), and *Tcf7l1^ΔN/ΔN* (33) have been previously described. We have previously shown that the *Hesx1-Cre* mouse line drives efficient recombination of loxP-flanked DNA in RP progenitors from 9.5 dpc (49, 50). *Hesx1^Cre/+;R26^loxP-YFP/+* 18.5 dpc embryos display widespread yellow fluorescent protein (YFP) expression in the vast majority of cells of the anterior pituitary, suggesting that the *Hesx1*-expressing RP progenitors give rise to all hormone-producing cells (*Hesx1*-cell lineage). In

addition to RP, *Hesx1^Cre/+;R26^loxP-YFP/+* and *Hesx1^Cre/+;R26^loxP-lacZl/+* embryos show reporter expression in the ventral telencephalon and preoptic hypothalamic area from 9.5 dpc (49–51). *Tcf7l1* is expressed in the forebrain, including the hypothalamic area, as well as in the anterior pituitary until 14.5 dpc (37). To reveal the function of *Tcf7l1* during normal HP axis development, we used the *Tcf7l1^flox/flox* conditional mouse line (44, 47). To generate pituitary-specific *Tcf7l1* genetic deletions, *Tcf7l1^flox/flox* mice were initially
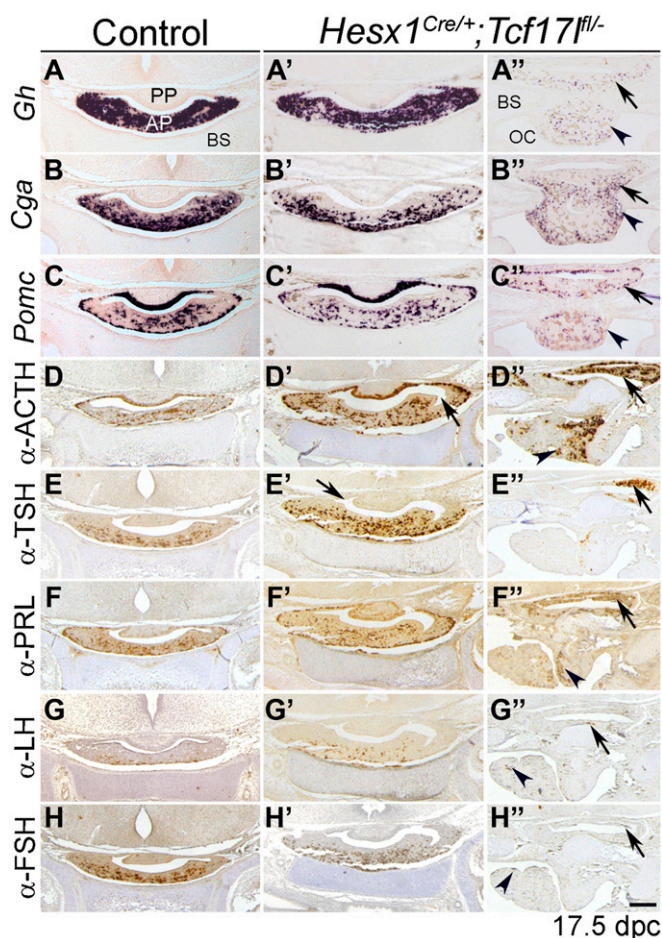

Fig. 1. Abnormal pituitary morphogenesis in *Hesx1^Cre/+;Tcf7l1^fl/−* mutants. In situ hybridization (A–C) and immunohistochemistry (D–H) of transverse histological sections of the pituitary gland of control embryos (A–H) and *Hesx1^Cre/+;Tcf7l1^fl/−* mutants (A′–H′ and A″–H″) at 17.5 dpc. (A′–H′) Mildly affected embryos show pituitary hyperplasia and cleft bifurcations (arrows in D′ and E′) but mostly normal expression of differentiation markers. (A″–H″) Severely affected pituitaries exhibit dysmorphic pituitary tissue that is ectopically located in the oropharyngeal cavity (arrowheads), but hormone-producing cells are present. AP, anterior pituitary; BS, basisphenoid bone; *Cga*, glycoprotein hormone α; *Gh*, growth hormone; OC, oral cavity; *Pomc1*, pro-opiomelanocortin-α; PP, posterior pituitary. Pictures are representative of five embryos per genotype. (Scale bar: H″, 100 μm.)

www.manaraa.com

crossed to β-actin:Cre animals (52) to generate *Tcf7l1*^{+/−} heterozygous mice. These mice were subsequently crossed to *Hesx1*[Cre/+] to generate *Hesx1*[Cre/+]; *Tcf7l1*^{+/−} double heterozygotes, which upon crossing with *Tcf7l1*[flox/flox] mice, were used to generate the *Hesx1*[Cre/+];*Tcf7l1*[flox/−] mice and embryos analyzed in this study. Genotyping of mice and embryos was carried out by PCR on ear punch biopsies or pieces of tissue from embryos digested in DNAreleasy (Anachem) as per manufacturer's instructions. The data presented in this work are representative of examples of at least three individual embryos per genotype. All of the experiments performed in mice were carried out according to UK Home Office guidance and approved by a local ethics committee.

Patient Recruitment. Patients with CH disorders were recruited into the study from both national and international pediatric and adult endocrinology centers between 1998 and 2005. A total of 215 probands (129 male, 86 female) were screened for mutations within *TCF7L1*. These included 31 patients with CH without any midline or eye defects, 6 with holoprosencephaly (HPE), 148 patients with SOD (characterized by optic nerve hypoplasia in association with hypopituitarism and/or midline defects), and 30 patients with anophthalmia ($n = 12$) or microphthalmia ($n = 18$). Ethics committee approval was obtained from the Institute of Child Health/Great Ormond Street Hospital for Children Joint Research Ethics Committee (Institute of Child Health, London, United Kingdom). Informed written consent was obtained from the parents and, where applicable, the patients before collection of samples and genomic analysis.

Mutation Analysis of *TCF7L1*. The entire coding region of *TCF7L1* (NM_031283) was PCR-amplified and subjected to direct-sequencing in our cohort. Detailed PCR and sequencing conditions are in *SI Materials and Methods*. For any mutations identified, control databases were consulted, including 1000 Genomes (www.1000genomes.org), Single Nucleotide Polymorphism Database (dbSNP), Exome Variant Server (EVS), and the Exome Aggregation Consortium (ExAC) (comprising >61,000 genomes) Browser (exac.broadinstitute.org). Patients 1 and 2 were screened and found not to carry mutations in other relevant genes involved in CH and SOD, specifically patient 1 was screened for mutations in *HESX1*, *CHD7*, *KAL1*, *PROKR2*, *FGFR1*, and *FGF8*; and patient 2 was screened for mutations in *HESX1*, *SOX3*, *KAL1*, *PROKR2*, *FGFR1*, and *FGF8*.

In Situ Hybridization on Histological Sections. Histological processing of embryos and in situ hybridization on paraffin sections was performed as previously described (53, 54). The antisense riboprobes used in this study [*Gh*, glycoprotein hormone α (*Cga*), *Pomc1*, *Prop1*, *Lh*, *Tsh*, *Fgf10*, *Fgf8*, *Bmp4*, LIM homeobox protein 3 (*Lhx3*), *Bmp4*, T-box 2 (*Tbx2*), T-box 3 (*Tbx3*), and *Pit1*] have been described (51, 53–55). Human *TCF7L1* riboprobe was generated using a full-length cDNA cloned into pCMV-Sport6 (SalI 5′, NotI 3′) (clone no. IRATp970D0681D, IMAGE no. 6141641; SourceBioscience).

Immunohistochemistry. Embryos were fixed in 4% (wt/vol) paraformaldehyde and processed for immunodetection as previously described (11, 51). Detection of hormones was carried out using antibodies for (α-ACTH) (10C-CR1096M1), α-TSH (NHPP AFP-1274789), α-PRL (NHPP AFP-425-10-91), α-LH (NHPP AFP-C697071P), and α-FSH (AFP-7798-1289) (Developmental Studies Hybridoma Bank) at a 1:1,000 dilution. α-SHH (AF464; R&D Systems) and α-TCF7L1 (33) were used at a 1:100 dilution and signal amplified using the Tyramide Signal Amplification kit (NEL741001KT; Perkin-Elmer). α-Cleaved Caspase 3 was used at a 1:300 dilution (9661; Cell Signaling Technologies) and α-phosphorylated-histone H3 at a 1:1,000 dilution (06-570; Upstate). The mitotic index of pituitary periluminal progenitors represents the percentage
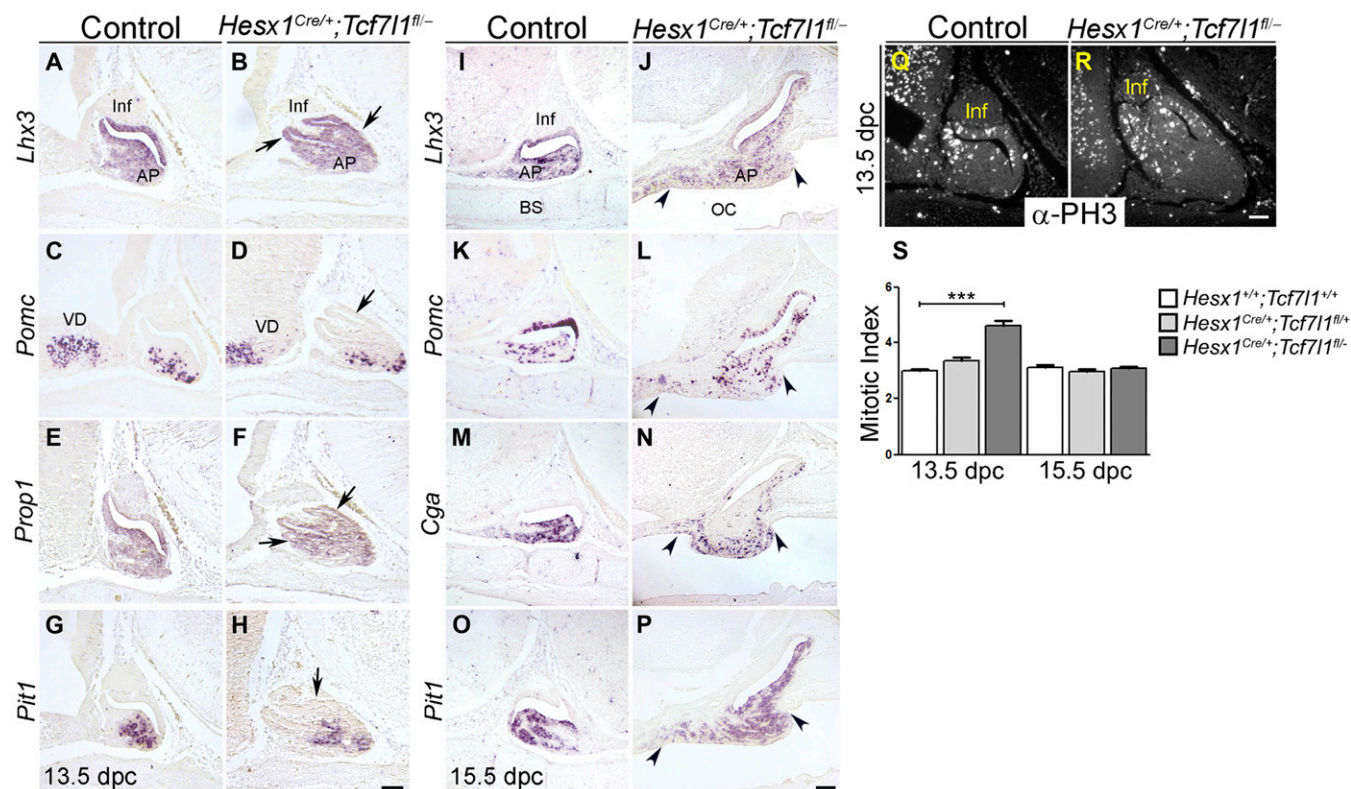

Fig. 2. Increased proliferation of RP progenitors but normal patterning of the developing anterior pituitary in *Hesx1*[Cre/+];*Tcf7l1*[fll/−] mutants. (*A–P*) In situ hybridization on sagittal sections through the pituitary gland of control and *Hesx1*[Cre/+];*Tcf7l1*[fll/−] mutant embryos (stage and probes are indicated; anterior to the left). (*A–H*) Mildly affected pituitaries show bifurcations and moderate expansion of the expression domains of *Lhx3* and *Prop1* at 13.5 and 15.5 dpc (arrows). (*I–P*) Severely affected pituitaries exhibit enlarged expression domains attributable to the abnormal morphogenesis of the developing anterior pituitary, which extends into the oropharyngeal cavity (arrowheads). (*Q–R*) Anti–phospho-histone H3 immunofluorescent staining on sagittal histological sections of a control embryo and a *Hesx1*[Cre/+];*Tcf7l1*[fll/−] mutant. (*S*) Quantitative analyses showing a statistically significant increase in the mitotic index in the *Hesx1*[Cre/+];*Tcf7l1*[fll/−] developing pituitaries relative to control littermates at 13.5 dpc but not at 15.5 dpc. AP, anterior pituitary; BS, basisphenoid bone; Inf, infundibulum; OC, oropharyngeal cavity. Pictures are representative of seven embryos per genotype. ***$P < 0.05$ (one-way ANOVA). (Scale bar: *H* and *P*, 100 μm.)
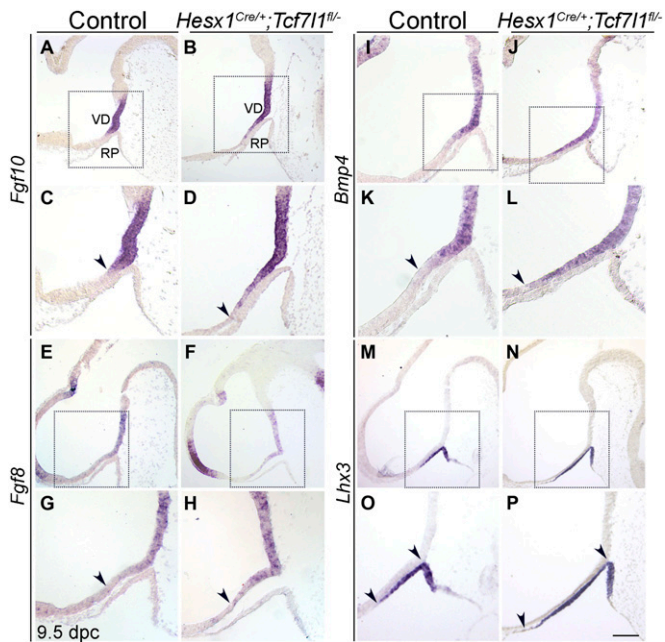
Fig. 3. Dysregulation of *Fgf8*, *Fgf10*, and *Bmp4* expression in the hypothalamus of *Hesx1*[Cre/+];*Tcf7l1*^{fl/−} mutants. In situ hybridization on sagittal histological sections revealing the expression of *Fgf10* (*A–D*), *Fgf8* (*E–H*), and *Bmp4* (*I–L*) in the prospective hypothalamus and *Lhx3* (*M–P*) in RP (anterior to the left). (*A–H*) *Fgf10* and *Fgf8* expression domains are anteriorized along the neural epithelium of the ventral diencephalon (i.e., prospective hypothalamus) overlaying the oral ectoderm of RP in the *Hesx1*[Cre/+];*Tcf7l1*^{fl/−} mutants (compare arrowheads in *C* and *D* and *G* and *H*, respectively). *C* and *D* and *G* and *H* represent enlarged images of the dotted squared areas in *A* and *B* and *E* and *F*, respectively. (*I–L*) The expression domain of *Bmp4* is rostrally expanded in *Hesx1*[Cre/+];*Tcf7l1*^{fl/−} prospective hypothalamus compared with control embryos (compare arrowheads *K* and *L*). *K* and *L* represent enlarged images of the squared dotted areas in *I* and *J*. (*M–P*) The expression domain of *Lhx3* is rostrally extended in *Hesx1*[Cre/+];*Tcf3*^{fl/−} compared with the control embryo (arrows in *O* and *P*), indicating an expansion of the RP epithelium. *O* and *P* are enlarged images of the dotted square areas in *M* and *N* respectively. VD, ventral diencephalon. Pictures are representative of five embryos per genotype. (Scale bar: *P*, 100 μm.)

of proliferating cells (phosphorylated histone H3-positive cells) from total number of DAPI-positive nuclei. Anti-phosphorylated histone H3 (1:1,000) (rabbit polyclonal; Upstate) was used for this study.

Cell Transfection, Luciferase Assays, and Immunoblotting. HEK293T cells were grown in DMEM supplemented with 10% FBS. Two reporters were used to assess the repressing activity of human wild-type TCF7L1 and the p.R92P and p.R400Q variants: (*i*) the TOPflash reporter plasmid carrying six wild-type binding sites for the TCF/LEF1 factors upstream of the firefly luciferase gene; (*ii*) the LEF1-promoter-luc reporter, which contains a DNA fragment (−6713 to −1 bp) of the human *LEF1* promoter inserted upstream of a luciferase reporter gene (33). Approximately 250,000 cells were seeded per well of 24-well tissue culture plates and the following day subjected to DNA transfection. A total of 100 ng of TOPflash or 200 ng of LEF1-promoter-luc reporter were cotransfected with constructs expressing wild-type and mutant hTCF7L1 proteins (10 and 50 ng) and 80 ng of Renilla luciferase plasmid as internal control using Lipofectamine 2000 (Life Technologies) according to the manufacturer's protocol. The total amount of DNA was kept constant in all of the transfections by complementing with pBluescript plasmid up to 350 ng. Activation of the TOPflash reporter was achieved by culturing the cells in the presence of 10 μM SB216763 (Sigma), a potent GSK3-β inhibitor, resulting in the stabilization of β-catenin. The LEF1-promoter-luc was activated with 30 μM SB216763. The repressing activity of wild-type hTCF7L1 and the variants was assessed 48 h posttransfection using the Dual-Luciferase Reporter Assay System (Promega) following the manufacturer's instructions. Total levels of repression caused by the hTCF7L1 p.R92P and p.R400Q proteins were represented as a percentage of the maximum repression caused by wild-type hTCF7L1. Experi-

ments were repeated four times in triplicates and statistical analysis was done using one-way ANOVA with Tukey's post hoc analysis.

Zebrafish Experiments. Zebrafish were bred and raised under standard conditions. *hdl/tcf7l1a*[m881−/−];*tcf7l1b*[zf157Tg+/−] (from now on *tcf7l1a*^{−/−}; *tcf3l1b*^{+/−}) zebrafish embryos were generated from crossing *tcf7l1a*^{+/−};*tcf7l1b*^{+/−} males with *tcf7l1a*^{+/−} females (56), raised at 28 °C and staged according to Kimmel et al. (57) Embryos were microinjected with 100 pg (5 nanoliters) of mRNA encoding either wild-type, p.R92P, or p.R400Q hTCF7L1 at one to two cell stage. mRNA encoding wild-type or mutant hTCF7L1 proteins was coinjected with mRNA encoding GFP, and embryos with low or no GFP fluorescence were excluded from the analysis. *tcf7l1a* alleles were genotyped by KASP assays (LCG Group). The *tcf7l1b* viral insertion was identified by genomic DNA PCR using the following primers: GSP2 forward, 5′-GGATACCGTGTGATCGTTTCTC-3′; and LTR2 reverse, 5′-TCTGTTCCTGACCTTGATCTGA-3′.

Statistics. Mendelian ratios were evaluated using the χ^2 test. For the luciferase assays, a one-way ANOVA was used, and for the zebrafish experiments, an unpaired *t* test was conducted. Values less than 0.05 were considered statistically significant. Quantitative data are presented as means ± SEM. Clonogenic potential of control and *Hesx1*[Cre/+];*Tcf7l1*^{+/−} mutant stem cells was evaluated using a paired *t* test. Total cell counts of control and *Hesx1*[Cre/+];*Tcf7l1*^{+/−} mutant pituitaries were analyzed by unpaired *t* test.

Results

Hesx1[Cre/+];*Tcf7l1*[flox/−] Mutants Exhibit Forebrain and Pituitary Defects.

Genotyping analysis of 9.5–18.5 dpc embryos from crosses between *Hesx1*[Cre/+];*Tcf7l1*^{+/−} and *Tcf7l1*[flox/flox] showed a normal Mendelian distribution of genotypes, implying that the lack of *Tcf7l1* in the *Hesx1* cell lineage is not embryonic lethal (Table 1). *Hesx1*[Cre/+]; *Tcf7l1*[flox/−] mutant embryos displayed variable degrees of anterior forebrain defects, including eye defects (i.e., microphthalmia or anophthalmia) and telencephalic abnormalities (i.e., small or
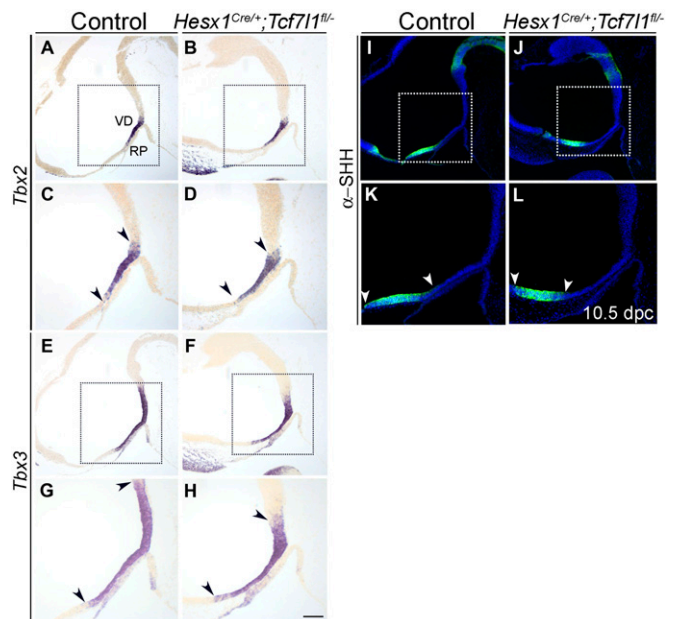

Fig. 4. SHH and its regulators *Tbx2* and *Tbx3* are misexpressed in the developing hypothalamus of *Hesx1*[Cre/+];*Tcf7l1*^{fl/−} mutants. (*A–H*) In situ hybridization on sagittal sections of 10.5-dpc embryos (anterior to the left) reveals the anterior shift of the *Tbx3* expression domain, and to a lesser extent *Tbx2*, within the developing hypothalamus of the *Hesx1*[Cre/+];*Tcf7l1*^{fl/−} mutants compared with the control embryos. (*I–L*) Immunostaining showing a reduction of SHH expression in the caudal region of the preoptic area in a *Hesx1*[Cre/+];*Tcf7l1*^{fl/−} mutant relative to a control. Note that the reduction of SHH expression in the caudal region of the preoptic area appears to overlap with the anterior extension of *Tbx3* expression. VD, ventral diencephalon. Pictures are representative of three embryos per genotype. (Scale bar: *P*, 100 μm.)

Gaston-Massuet et al.

absent telencephalic vesicles), as previously described (47) (Fig. S1C). Additionally, we observed neural tube closure defects resulting in exencephaly in around 10% of these mutants (Fig. S1B). Genotyping analyses of mice at 3 wk of age revealed no significant differences of the expected Mendelian ratios for the $Hesx1^{Cre/+}$; $Tcf7l1^{flox/-}$ mutants compared with control littermates, but perinatal death was observed in some $Hesx1^{Cre/+}$;$Tcf7l1^{flox/-}$ mice (Table 1). Most of the surviving mutants did not exhibit any gross morphological defects, but around 25% of these showed dwarfism with reduced size and weight compared with their littermates, suggesting a potential functional compromise of the HP axis (Fig. S1 A, D, and E). We observed unilateral microphthalmia with no compromise of the telencephalic vesicles in around 20% of the $Hesx1^{Cre/+}$; $Tcf7l1^{flox/+}$ embryos as previously reported (47).

Histological and in situ hybridization analyses of $Hesx1^{Cre/+}$; $Tcf7l1^{flox/-}$ mutant and control embryos at 17.5 dpc revealed two clearly discernable pituitary phenotypes. (i) Group 1 embryos, ~25% of the $Hesx1^{Cre/+}$;$Tcf7l1^{flox/-}$ mutants, displayed severe morphological defects and ectopic pituitary tissue was often observed in the roof of the oropharyngeal cavity (Fig. 1 A''–H''). In these mutants, morphologically distinguishable posterior or intermediate lobes could not be observed. This phenotype was associated with severe forebrain defects. Hormone-producing cells were detected in these mutants, even in the ectopically located pituitary tissue. (ii) Group 2 embryos, accounting for ~75% of $Hesx1^{Cre/+}$; $Tcf7l1^{flox/-}$ mutants, showed a less severe phenotype with mild pituitary hyperplasia and presence of pituitary cleft bifurcations (Fig. 1 D'–H'). Posterior and intermediate lobes appeared morphologically normal in mutants in this group. Total cell counting of dissociated pituitaries at 18.5 dpc revealed average cell counts of 75,300 ± 5,227.33 for the $Hesx1^{Cre/+}$;$Tcf7l1^{flox/-}$ mutants ($n = 5$) and 66,200 ± 7,585.62 for controls ($n = 8$). Although these differences did not reach statistical significance ($P = 0.0584$), the data suggest a trend toward mild hyperplasia in group 2 mutants.

Differentiation of hormone-producing cells occurred normally with no apparent differences between $Hesx1^{Cre/+}$;$Tcf7l1^{flox/-}$ group 2 mutants and control embryos. The Sox2-positive stem cell compartment was analyzed in vitro by culturing dissociated cells in stem cell-promoting medium, which revealed no differences in clonogenic potential between group 2 mutants and controls (Fig. S2).

Similar morphological abnormalities, including hyperplasia, cleft bifurcations, and ectopically located pituitary tissue, were observed in $Hesx1^{Cre/+}$;$Tcf7l1^{flox/-}$ mutants at 13.5 and 15.5 dpc. Nevertheless, expression of $Lhx3$, $Pomc1$, $Prop1$, and $Pit1$ at 13.5 dpc as well as $Lhx3$, $Pomc1$, Cga, and $Pit1$ at 15.5 dpc was detected in the developing pituitary of all mutants analyzed (Fig. 2 A–P). Together, these analyses suggest that loss of $Tcf7l1$ in $Hesx1$-expressing cells leads to aberrant pituitary morphogenesis but normal cell differentiation in the majority of the embryos, with low penetrance of a phenotype characterized by ectopic pituitary tissue, possibly of anterior lobe identity, in the oropharyngeal cavity concomitant with defective terminal differentiation.

Abnormal Hypothalamic Signaling and Increased Proliferation of Rathke's Pouch Progenitors in $Hesx1^{Cre/+}$;$Tcf7l1^{flox/-}$ Mutants. During early pituitary development, the synergistic expression of $Bmp4$, $Fgf8$, and $Fgf10$ within the developing hypothalamus is essential for the induction of $Lhx3$ in the region of the oral ectoderm fated to become RP (2). The expression domains of $Fgf8$, $Fgf10$, and $Bmp4$ in the hypothalamic anlage (Fig. 3 A–L) and of $Lhx3$ in the underlying RP (Fig. 3 M–P) were rostrally expanded in the $Hesx1^{Cre/+}$;$Tcf7l1^{flox/-}$ mutants relative to controls at 9.5 dpc. Enlargement of the $Lhx3$-expression domain suggests the recruitment of additional oral ectoderm into RP epithelium, which may contribute to the hyperplasia observed at subsequent developmental stages. The expression of SHH, another critical signal required for normal RP development (58, 59), in the
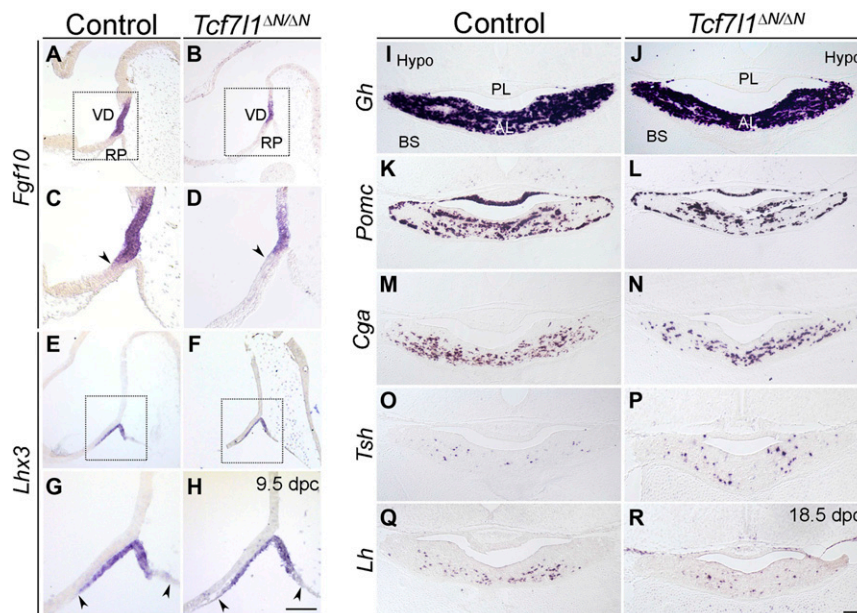

Fig. 5. Expression of a mutant form of TCF7L1 lacking the β-catenin-interacting domain ($Tcf7l1^{ΔN/ΔN}$) is sufficient to sustain normal hypothalamic-pituitary axis development. (A–H) In situ hybridization on sagittal sections showing normal expression domains of $Fgf10$ (A–D) and $Lhx3$ (E-H) in $Tcf7l1^{ΔN/ΔN}$ mutants and control wild-type littermates at 9.5 dpc (anterior to the left). C, D, G, and H are enlarged images of the dotted squared areas. The apparent difference in size in the $Tcf7l1^{ΔN/ΔN}$ mutants relative to the controls is caused by an overall developmental delay in the mutants. (I–R) In situ hybridization on transverse histological sections through the pituitary gland of $Tcf7l1^{ΔN/ΔN}$ mutants and control embryos at 18.5 dpc reveal no gross differences in the levels of expression of several differentiation markers. Note that pituitary morphogenesis is also normal in $Tcf7l1^{ΔN/ΔN}$ mutants relative to controls. AL, anterior lobe; BS, basisphenoid bone; PL, posterior lobe; VD, ventral diencephalon. Pictures are representative of five embryos per genotype. (Scale bars: H and R, 100 μm.)
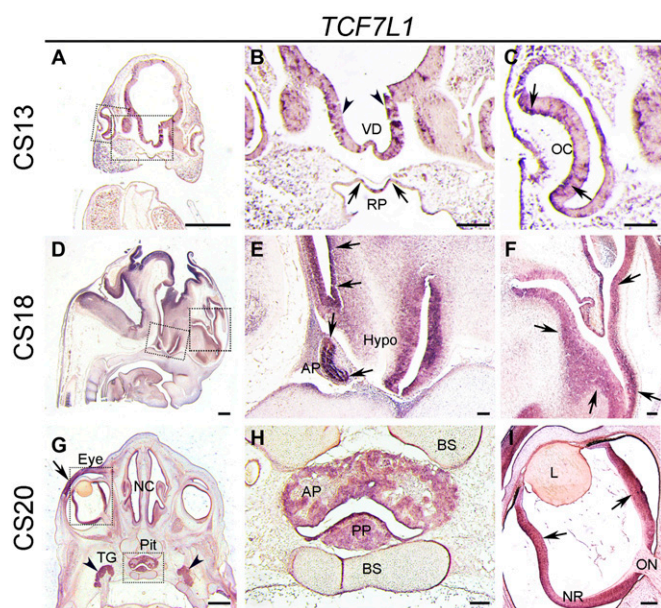
Fig. 6. *TCF7L1* is expressed in the developing hypothalamic-pituitary axis, central nervous system and eyes during human embryogenesis. In situ hybridization against *hTCF7L1* on coronal (*A–C* and *G–I*) or sagittal (*D–F*) histological sections at Carnegie stage (CS) 13, 18, and 20. (*A–C*) Note the expression of *hTCF7L1* in the ventral diencephalon neuroepithelium (i.e., prospective hypothalamus) (arrowheads in *B*), RP progenitors (arrows in *B*), and developing optic cups (arrows in *C*) at CS13. (*D–F*) At CS18, expression of *hTCF7L1* is observed throughout the neuroepithelium of the hind-, mid-, and forebrain, including the hypothalamus (arrowheads in *E*) and telencephalon (arrows in *F*). Expression is also detected in the developing anterior pituitary gland (arrows in *E*). (*G–I*) At CS20, expression of *hTCF7L1* is detected in the anterior and posterior lobes of the pituitary gland (*H*), neural retina (arrows in *I*), eyelid (arrow in *G*), olfactory epithelium of the nasal cavity, and trigeminal ganglia. *B*, *C*, *E*, *F*, *H*, and *I* are enlarged images of the dotted squared areas. AP, anterior pituitary; BS, basisphenoid bone; hyp, hypothalamus; NC, nasal cavity; NR, neural retina; OC, optic cup; ON, optic nerve; PP, posterior pituitary; VD, ventral diencephalon. (Scale bars: *A*, *D*, and *G*, 500 μm; *B*, *C*, *E*, *F*, *H* and *I*, 100 μm.)

preoptic area of the hypothalamus was shifted anteriorly and slightly reduced in the *Hesx1^{Cre/+}*;*Tcf7l1^{flox/−}* mutants in comparison with controls (Fig. 4 *I–L*). In agreement with this observation, the expression domains of *Tbx3* and to a lesser extent *Tbx2*, which normally act as repressors of *Shh* expression in the hypothalamus (55), were rostrally shifted, thus invading the caudal region of the preoptic area, where SHH expression appears reduced (Fig. 4 *A–H*).

Proliferation analysis revealed a mild but statistically significant increase in the mitotic index of RP periluminal progenitors in *Hesx1^{Cre/+}*;*Tcf7l1^{flox/−}* mutant pituitaries at 13.5 dpc ($P < 0.05$), but this increase was transient and not observed at 15.5 dpc ($P > 0.05$) (Fig. 2 *Q–S*). This phenotype is entirely consistent with the deletion of *Tcf7l1* in both the hypothalamus and RP in the *Hesx1^{Cre/+}*;*Tcf7l1^{flox/−}* mutant pituitaries (Fig. S3 *C* and *D*). Caspase 3 immunostaining revealed the presence of a few apoptotic cells in the ventral regions of RP in both the mutant and control embryos (Fig. S3 *A* and *B*). Together, these studies suggest that *Tcf7l1* is required for proper patterning of the prospective hypothalamus and for establishment of the normal expression domains of critical hypothalamic signals involved in the induction and proliferation of RP progenitors.

TCF7L1 Functions as a Repressor During Normal Pituitary Organogenesis. Next, we sought to assess whether the requirement of TCF7L1 within the developing hypothalamus and pituitary gland was dependent or independent of β-catenin. To achieve this, we used a recently generated mouse line (*Tcf7l1^{ΔN/ΔN}*) expressing a TCF7L1 mutant protein lacking the β-catenin–interacting domain at the N terminus. This truncated form of TCF7L1 (TCF7L1^{ΔN}) shows similar DNA–binding and -repressing activities to wild-type TCF7L1, but the mutant's interaction with β-catenin is abolished (33).

In situ hybridization analysis revealed the absence of morphological defects in the pituitary gland and the normal expression of terminal differentiation markers (*Gh*, *Pomc*, *Cga*, *Tsh*, and *Lh*) in *Tcf7l1^{ΔN/ΔN}* mutants relative to control embryos at 18.5 dpc (Fig. 5 *I–R*). Likewise, the expression domain of *Fgf10* within the hypothalamus and *Lhx3* in the developing RP were comparable between genotypes (Fig. 5 *A–H*). Note that *Tcf7l1^{ΔN/ΔN}* mutants show a general developmental delay and are smaller than control littermates, which accounts for the slight size differences in the expression domains (Fig. 5 *C* and *D*) (33). The absence of any apparent defects in *Tcf7l1^{ΔN/ΔN}* mutants demonstrates that TCF7L1 acts primarily as a transcriptional repressor within the developing hypothalamus and pituitary gland and that TCF7L1's function is independent of β-catenin. Additionally, these data imply that the defects observed in *Hesx1^{Cre/+}*; *Tcf7l1^{flox/−}* mutants are a consequence of the derepression of TCF7L1 transcriptional targets.

Variants in *TCF7L1* Are Associated with Forebrain and Pituitary Defects in Humans. The forebrain and pituitary defects observed in the *Hesx1^{Cre/+}*;*Tcf7l1^{flox/−}* mutants are very similar to those previously described in *Hesx1*-deficient embryos, suggesting that these

Table 2. Phenotypes in patients with *TCF7L1* variations

Patient	Variant	Sex	Age, y	Height, SD	Weight, SD	Endocrinopathy	MRI	Eyes
1	p.R92P	Male	0.5	−1.8	−2.3	Marginally low IGF1 10.6 nmol/L (normal range, 11–32 nmol/L); normal FT$_4$, TSH, and prolactin	Partial agenesis of CC; thin anterior commissure; right optic nerve thinner than left	Normal optic nerves; thin right optic tract; ERG normal
			9	−2.1	−2.4			
2	p.R400Q	Male	0.7	−1.23*	−2.2*	GHD [low IGF1 28 ng/mL (−2 SDs from normal range), IGFBP3 1.27 mg/L (−3 SDs; normal range, 1.107–3.825 mg/L), peak GH 3.4 μg/L]; normal FT$_4$ with mildly elevated TSH (6.2 mU/L); prolactin 618 mU/L	Absent PP, APH, and SP; small optic nerves and chiasm	Nystagmus; ONH

APH, anterior pituitary hypoplasia; CC, corpus callosum; ERG, electroretinogram; FT$_4$, free thyroxine; GHD, growth hormone deficiency; ONH, optic nerve hypoplasia; PP, posterior pituitary; SP, septum pellucidum.
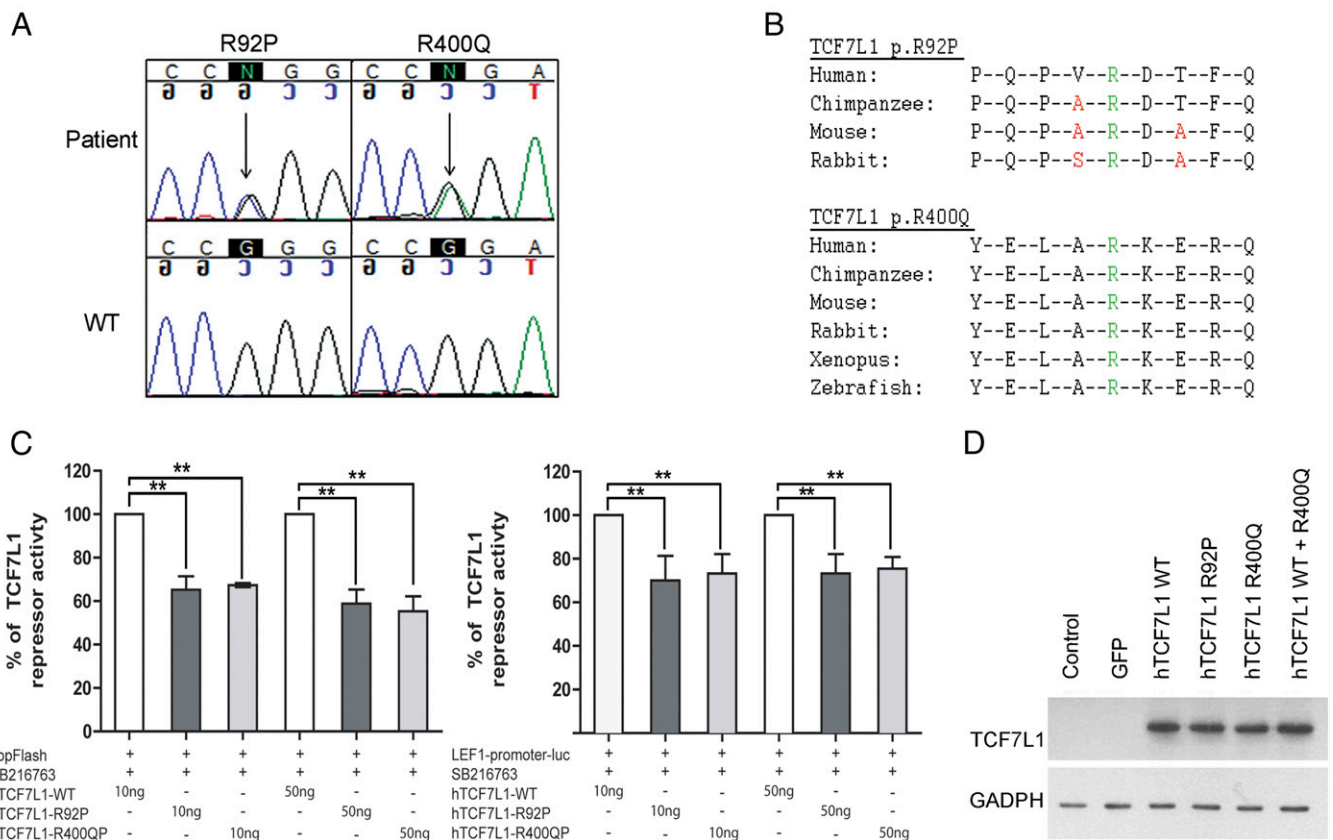
Gaston-Massuet et al.

Fig. 7. Identification of hTCF7L1 heterozygous missense variants in patients with SOD. (*A*) Electropherogram showing two heterozygous missense variants in hTCF7L1: p.R92P and p.R400Q. (*B*) Both DNA variants result in the substitution of highly conserved amino acids. R92 is not conserved in *Xenopus* and zebrafish. (*C*) Transient luciferase assays on HEK293 cells cotransfected with either TOPflash (left graph) or *hLEF1*-promoter-luc (right graph) reporters and constructs expressing wild-type, p.R92P, or p.R400Q hTCF7L1 proteins. Note the significant reduction in repressing activity of the p.R92P and p.R400Q hTCF7L1 variants relative to wild-type TCF7L1 using both reporters. **$P < 0.05$ (one-way ANOVA). (*D*) Western blot analysis of transfected HEK293 cells used in *C* with a specific anti-TCF7L1 antibody detects the expression of the wild-type and p.R92P or p.R400Q hTCF7L1 proteins at similar levels. GAPDH was also detected in the same membrane as loading control.

transcriptional repressors may control the same genetic program (49, 54). Because mutations in *HESX1* have been associated with congenital hypopituitarism in humans, including SOD (60, 61), we hypothesized that mutations in *TCF7L1* may also be implicated in these conditions. Indeed, in situ hybridization showed that *TCF7L1* is expressed during human embryonic development within brain tissue, including the hypothalamus, and the developing pituitary gland (Fig. 6).

To investigate this possibility, we screened a total of 215 patients with hypopituitarism including SOD for mutations in the *TCF7L1* locus by Sanger sequencing. Two heterozygous sequence variants resulting in amino acid changes in highly conserved residues of TCF7L1 were identified in two unrelated patients (clinical details are presented in Table 2 and *SI Text*).

Patient 1 of Caucasian (Finnish; nonconsanguineous) descent, showing forebrain defects (i.e., partial agenesis of the corpus callosum, thin right optic tract, and thin anterior commissure), and normal pituitary function, carried a missense G-to-C sequence variant at position 275 (c.275G > C), which causes the substitution of arginine 92 by proline (p.R92P) (Fig. 7 *A* and *B*). This variant was not identified in online databases (listed in *Materials and Methods*) or 392 additional Caucasian controls (including 200 healthy Finnish). The variant was inherited from the father and was also present in the paternal uncle, who were both asymptomatic.

Patient 2, of Pakistani (nonconsanguineous) descent, was diagnosed with classic SOD and showed small optic nerves and

chiasm, an absent posterior pituitary, a very small anterior pituitary and absent septum pellucidum. The proband harbored a missense G-to-A sequence variant (c.1199G > A), resulting in an arginine to glutamine change at position 400 (p.R400Q) (Fig. 7 *A* and *B*). Although this variant was not identified in our healthy controls or the dbSNP or the Exome Sequencing Project (ESP) databases, the variant is present in 14 individuals in the ExAC database with an allelic frequency of $2.958 \times e^{-5}$ in heterozygosity. The variant was inherited from the unaffected mother, and two unaffected siblings also carried the variant.

TCF7L1 p.R92P and p.R400Q Variants Show Impaired Repressing Activity in Vitro and in Vivo. We sought to assess the capacity of wild-type and hTCF7L1 p.R92P and p.R400Q proteins to repress WNT/β-catenin-mediated transcriptional activation in vitro. We used two different reporters in transfected HEK293 cells cultured in the presence of a GSK3β inhibitor. Using the TOPflash reporter, the repressing activity of the TCF7L1 (p.R92P) variant was reduced by 34–40% (10 ng and 50 ng, respectively; $P < 0.05$) relative to wild-type TCF7L1 (Fig. 7*C*, left graph). Likewise, the repressing activity of the TCF7L1 (p.R400Q) variant on the TOPflash reporter was diminished by 41–55% (10 ng and 50 ng, respectively; $P < 0.05$) compared with wild-type TCF7L1 (Fig. 7*C*, left graph). A reduction of the transcriptional repressing activity of these variants was also observed when using the *hLEF1*-promoter-luc reporter [30% reduction for TCF7L1 (p.R92P) and 27% reduction for the TCF7L1 (p.R400Q) ($P < 0.05$); Fig. 7*C*, right
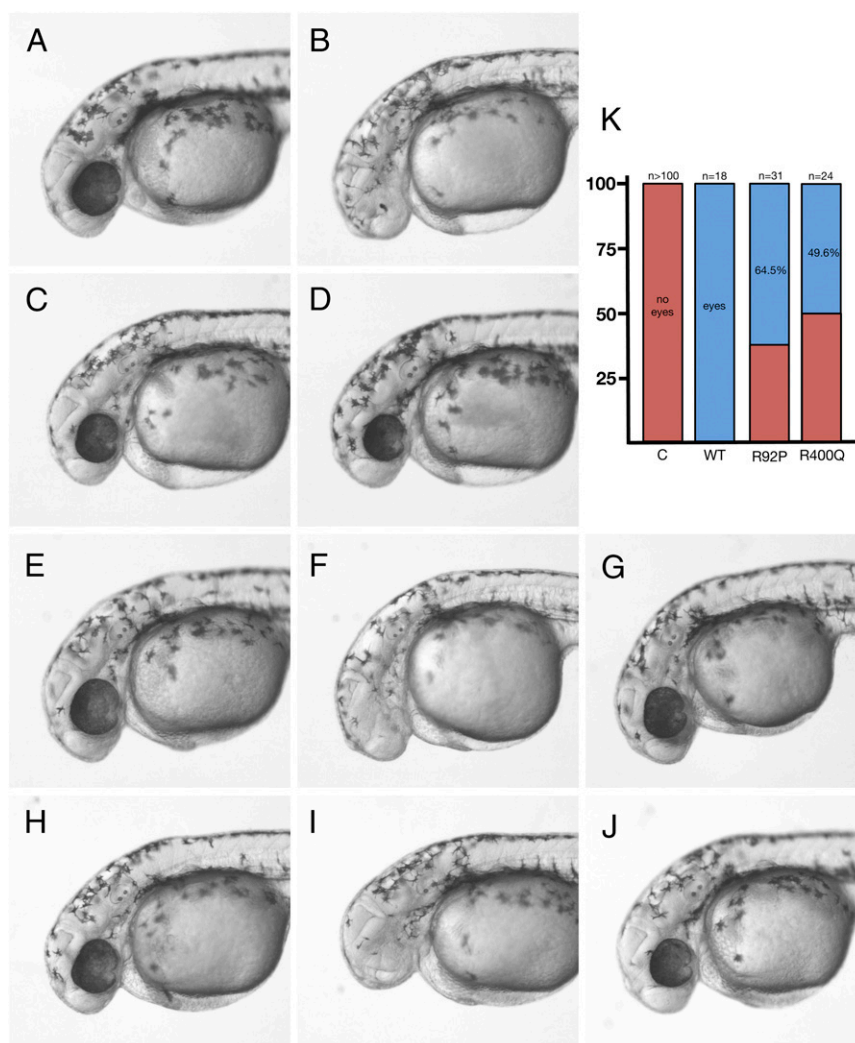
Gaston-Massuet et al.

www.manaraa.com

Fig. 8. Incomplete rescue of the eyeless phenotype of double *tcf7l1a/b* zebrafish mutants with the human hTCF7L1 p.R92P and p.R400Q variants. Lateral view of 32-h postfertilization zebrafish embryos (anterior to left). Wild-type embryos injected with 100 pg of *hTCF7L1* (*C*), *p.R92P* (*E*), and *p.R400Q* (*H*) mRNA show no phenotype compared with wild-type untreated embryos (*A*). *tcf7l1a⁻/⁻;tcf3l1b⁺/⁻* double mutants fail to develop eyes (*B*). Injection of *tcf7l1a⁻/⁻; tcf3l1b⁺/⁻* double mutants with 100 pg of wild-type *hTCFL1* mRNA rescues the eyeless phenotype (*D*). Injection of *tcf7l1a⁻/⁻;tcf3l1b⁺/⁻* double mutants with 100 pg of *hTCF7L1 p.R92P* (*F* and *G*) or *p.R400Q* (*I* and *J*) results in incomplete rescue of the eyeless phenotype. (*K*) Percentage of embryos with normal eyes is shown in blue, and percentage of embryos with very small or no eyes is shown in red. p.R92P: 64.5% SD 12.41, P < 0.009; p.R400Q: 49.65% SD 5.93, P < 0.0006 (unpaired t test).

graph]. In these transfection experiments, wild-type and mutant hTCF7L1 proteins were expressed at similar levels, as revealed by Western blot analysis using a specific anti-TCF7L1 antibody (Fig. 7*D*). A potential molecular mechanism underlying the decreased repressing activity of the TCF7L1 (p.R92P) variant could be the increased phosphorylation of this protein by the Homeodomain-Interacting Protein Kinase 2 (HIPK2) compared with wild-type hTCF7L1 (Fig. S4 and *SI Text*). No dominant-negative effects were observed in cotransfection experiments combining wild-type and hTCF7L1 p.R92P and p.R400Q variants (Fig. S5).

Finally, to assess the repressing activities of the two variants in vivo, we took advantage of a zebrafish model with a lower gene dosage of the *hTCF7L1* orthologs *tcf7l1a* and *tcf7l1b*. *tcf7l1a⁻/⁻* and *tcf3l1b⁺/⁻* single mutants show no phenotype, but *tcf7l1a⁻/⁻; tcf3l1b⁺/⁻* double mutants exhibit an eyeless phenotype attributable to the ectopic activation of the Wnt/β-catenin signaling pathway and derepression of targets of this pathway in the forebrain (including the eye field) (30, 31). We injected double

tcf7l1a⁻/⁻;tcf7l1b⁺/⁻ double mutant zebrafish embryos, which normally develop no eyes, with mRNA encoding either wild-type hTCF7L1 or the two variants identified, with the aim of determining the variants' ability to rescue the eyeless phenotype. Microinjection of wild-type *hTCF7L1* mRNA fully rescued the eyeless phenotype of *tcf7l1a⁻/⁻;tcf3l1b⁺/⁻* double mutants (Fig. 8; n = 18 mutants, three independent experiments). However, only 64.5% (n = 31 mutants, three independent experiments) and 49.65% (n = 24 mutants, two independent experiments) of the eyeless *tcf7l1a⁻/⁻;tcf3l1b⁺/⁻* double mutants were rescued by injection of mRNA encoding the hTCF7L1 p.R92P and p.R400Q variants, respectively (Fig. 8). These results support the in vitro findings previously presented and add further evidence to the notion that the hTCF7L1 variants p.R92P and p.R400Q exhibit reduced repressing activity in vivo.

Discussion

In this study, we have provided genetic and molecular evidence demonstrating that the repressing activity of the transcription

Gaston-Massuet et al.

factor TCF7L1 is required for normal establishment of the HP axis in mice and humans.

The pituitary defects of the $Hesx1^{Cre/+};Tcf7l1^{flox/-}$ mouse mutants are very similar to those observed in $Hesx1^{-/-}$ embryos; increased proliferation leading to abnormal pituitary morphogenesis but overall normal terminal differentiation (14, 54). We show the absence of mTCF7L1 protein in both the hypothalamus and the developing RP by 10.5 dpc in $Hesx1^{Cre/+};Tcf7l1^{fl/-}$ mutants, thus validating the genetic approach. Within the hypothalamus, we have revealed a critical role for mTCF7L1 in the regulation of anteroposterior patterning, because there is an overall anterior shift in the expression domains of caudal hypothalamic signals and markers (e.g., *Fgf8*, *Fgf10*, *Bmp4*, *Tbx2*, and *Tbx3*), which is concomitant with a reduction in SHH expression in the anterior hypothalamic area (Figs. 3 and 4). This abnormal hypothalamic signaling results in the recruitment of additional ectoderm into RP, as detected by the rostral expansion in the *Lhx3* expression domain and increased proliferation in the developing pituitary of $Hesx1^{Cre/+};Tcf7l1^{fl/-}$ mutants at 13.5 dpc. In addition, there may be a contribution to the phenotype attributable to the lack of TCF7l1 within RP, which we cannot rule out.

There is a marked variability of expressivity of the pituitary phenotype in $Hesx1^{Cre/+};Tcf7l1^{fl/-}$ mouse mutants (Figs. 1 and 2), which is reminiscent of that observed in *Hesx1*-deficient embryos. In most of the $Hesx1^{Cre/+};Tcf7l1^{fl/-}$ mutants (group 2), there is an overall increase in pituitary tissue, and anterior, posterior, and intermediate lobes can be identified. However, in the most severely affected mutants (group 1), the posterior and intermediate lobes cannot be morphologically detected from 13.5 to 17.5 dpc. Incidentally, some $Hesx1^{Cre/+};Tcf7l1^{fl/-}$ mutants at 9.5 dpc show a lack of contact between the developing infundibulum and RP, which may contribute to the development of the ectopic pituitary in the roof of the oropharyngeal cavity. It is likely that this phenotypic variability observed from 13.5 dpc is brought about by the differential dysregulation of the hypothalamic signals normally involved in induction and proliferation of RP progenitors, an idea that is difficult to test experimentally.

Previously, we have shown that the cooperation between HESX1 and TCF7L1 is required to repress the activation of the WNT/β-catenin pathway in the anterior neural plate of zebrafish and mouse embryos (47). Our data are in support of the idea that TCF7L1 acts as a repressor during normal pituitary development in mice. Functional studies in mice have demonstrated a temporally specific function of the WNT/β-catenin signaling pathway during pituitary organogenesis. This pathway must be repressed at early stages of pituitary development and activated from 14.5 dpc for normal differentiation of the *Pou1f1*-cell lineage (37). In agreement with this notion, the permanent activation of the WNT/β-catenin pathway in RP progenitors at 9.5 dpc, by expression of a degradation-resistant form of β-catenin, results in severe pituitary hyperplasia during embryogenesis (50). Mice deficient for *Tcf7l2*, a TCF/LEF factor shown to act as either an activator or a repressor depending on the cell context, show anterior pituitary hyperplasia but no defects in the differentiation

of hormone-producing cells (41). The similarities in the pituitary phenotype between $Tcf7l2^{-/-}$, $Hesx1^{-/-}$, and $Hesx1^{Cre/+};Tcf7l1^{flox/-}$ mutants suggest that these factors are likely to act as transcriptional repressors of WNT/β-catenin pathway targets during HP axis development. Indeed, the expression of a mutant form of TCF7L1 unable to interact with β-catenin, but maintaining repressing activity does not lead to any hypothalamic or pituitary defects, demonstrating that TCF7L1 is required as a repressor (Fig. 5).

Our data also provide evidence that the repressing activity of TCF7L1 is required for normal HP axis development in humans. Firstly, we show the expression of *hTCF7L1* mRNA in the developing human embryo (Fig. 6). Furthermore, we have identified two TCF7L1 variants, p.R92P and p.R400Q, in unrelated families with SOD, which substitute highly conserved residues, and have shown that these variants are functionally compromised. These mutant proteins show reduced repressing activity relative to wild-type TCF7L1 using both the TOPflash reporter plasmid and a luciferase reporter containing a fragment of the human *LEF1* promoter (Fig. 7) (33). In addition, we show that the TCF7L1 p.R92P and p.R400Q variants cannot rescue the eye defects of zebrafish mutants with a reduced gene dosage of *tcf7l1* (Fig. 8). Given the presence of the variants in the phenotypically unaffected father and paternal uncle, our data suggest that the variants are not uniquely responsible for disease development but may be variably penetrant. The concept of variable penetrance has been observed in a variety of human genetic disorders. These disorders include Kallmann syndrome, where recent data have suggested an oligogenic basis to the disorder (62). Additionally, mutations in SHH and *GLI2*, a mediator of SHH, are associated with variably penetrant holoprosencephaly. Sequence variants in *LHX4* and *GLI2* are also associated with variably penetrant CH (63, 64). Of note, variable phenotypic expressivity is also observed in the $Hesx1^{Cre/+};Tcf7l1^{fl/-}$ mouse mutants and in the $tcf7l1a^{-/-};tcf3l1b^{+/-}$ zebrafish mutants injected with the hTCF7L1 variants identified in this study.

In summary, we identify *Tcf7l1* as a determinant for the establishment of the HP axis and as a potential candidate gene to be mutated in congenital hypopituitarism.

1. Castinetti F, et al. (2014) Combined pituitary hormone deficiency: Current and future status. *J Endocrinol Invest* 38(1):1–12.
2. Kelberman D, Rizzoti K, Lovell-Badge R, Robinson IC, Dattani MT (2009) Genetic regulation of pituitary gland development in human and mouse. *Endocr Rev* 30(7): 790–829.
3. Alatzoglou KS, Dattani MT (2010) Genetic causes and treatment of isolated growth hormone deficiency-An update. *Nat Rev Endocrinol* 6(10):562–576.
4. Bancalari RE, Gregory LC, McCabe MJ, Dattani MT (2012) Pituitary gland development: An update. *Endocr Dev* 23:1–15.
5. Davis SW, et al. (2010) Molecular mechanisms of pituitary organogenesis: In search of novel regulatory genes. *Mol Cell Endocrinol* 323(1):4–19.
6. Mollard P, Hodson DJ, Lafont C, Rizzoti K, Drouin J (2012) A tridimensional view of pituitary development and function. *Trends Endocrinol Metab* 23(6): 261–269.

7. Bilodeau S, Roussel-Gervais A, Drouin J (2009) Distinct developmental roles of cell cycle inhibitors p57Kip2 and p27Kip1 distinguish pituitary progenitor cell cycle exit from cell cycle reentry of differentiated cells. *Mol Cell Biol* 29(7):1895–1908.
8. Davis SW, Mortensen AH, Camper SA (2011) Birthdating studies reshape models for pituitary gland cell specification. *Dev Biol* 352(2):215–227.
9. Prince KL, Walvoord EC, Rhodes SJ (2011) The role of homeodomain transcription factors in heritable pituitary disease. *Nat Rev Endocrinol* 7(12):727–737.
10. Castinetti F, Davis SW, Brue T, Camper SA (2011) Pituitary stem cell update and potential implications for treating hypopituitarism. *Endocr Rev* 32(4):453–471.
11. Andoniadou CL, et al. (2013) Sox2(+) stem/progenitor cells in the adult mouse pituitary support organ homeostasis and have tumor-inducing potential. *Cell Stem Cell* 13(4):433–445.
12. Rizzoti K, Akiyama H, Lovell-Badge R (2013) Mobilized adult pituitary stem cells contribute to endocrine regeneration in response to physiological demand. *Cell Stem Cell* 13(4):419–432.

13. Brickman JM, et al. (2001) Molecular effects of novel mutations in Hesx1/HESX1 associated with human pituitary disorders. *Development* 128(24):5189–5199.

14. Dasen JS, et al. (2001) Temporal regulation of a paired-like homeodomain repressor/TLE corepressor complex and a related activator is required for pituitary organogenesis. *Genes Dev* 15(23):3193–3207.

15. Clevers H, Nusse R (2012) Wnt/β-catenin signaling and disease. *Cell* 149(6):1192–1205.

16. Moon RT, Bowerman B, Boutros M, Perrimon N (2002) The promise and perils of Wnt signaling through beta-catenin. *Science* 296(5573):1644–1646.

17. MacDonald BT, Tamai K, He X (2009) Wnt/beta-catenin signaling: Components, mechanisms, and diseases. *Dev Cell* 17(1):9–26.

18. Aberle H, Bauer A, Stappert J, Kispert A, Kemler R (1997) beta-catenin is a target for the ubiquitin-proteasome pathway. *EMBO J* 16(13):3797–3804.

19. Liu C, et al. (2002) Control of beta-catenin phosphorylation/degradation by a dual-kinase mechanism. *Cell* 108(6):837–847.

20. Behrens J, et al. (1998) Functional interaction of an axin homolog, conductin, with beta-catenin, APC, and GSK3beta. *Science* 280(5363):596–599.

21. Ikeda S, et al. (1998) Axin, a negative regulator of the Wnt signaling pathway, forms a complex with GSK-3beta and beta-catenin and promotes GSK-3beta-dependent phosphorylation of beta-catenin. *EMBO J* 17(5):1371–1384.

22. Sharpe C, Lawrence N, Martinez Arias A (2001) Wnt signalling: A theme with nuclear variations. *BioEssays* 23(4):311–318.

23. Roose J, et al. (1998) The Xenopus Wnt effector XTcf-3 interacts with Groucho-related transcriptional repressors. *Nature* 395(6702):608–612.

24. van Beest M, et al. (2000) Sequence-specific high mobility group box factors recognize 10-12-base pair minor groove motifs. *J Biol Chem* 275(35):27266–27273.

25. van de Wetering M, Clevers H (1992) Sequence-specific interaction of the HMG box proteins TCF-1 and SRY occurs in the minor groove of a Watson-Crick double helix. *EMBO J* 11(8):3039–3044.

26. Brantjes H, Roose J, van De Wetering M, Clevers H (2001) All Tcf HMG box transcription factors interact with Groucho-related co-repressors. *Nucleic Acids Res* 29(7):1410–1419.

27. Eastman Q, Grosschedl R (1999) Regulation of LEF-1/TCF transcription factors by Wnt and other signals. *Curr Opin Cell Biol* 11(2):233–240.

28. van Genderen C, et al. (1994) Development of several organs that require inductive epithelial-mesenchymal interactions is impaired in LEF-1-deficient mice. *Genes Dev* 8(22):2691–2703.

29. Zhou P, Byrne C, Jacobs J, Fuchs E (1995) Lymphoid enhancer factor 1 directs hair follicle patterning and epithelial cell fate. *Genes Dev* 9(6):700–713.

30. Dorsky RI, Itoh M, Moon RT, Chitnis A (2003) Two tcf3 genes cooperate to pattern the zebrafish brain. *Development* 130(9):1937–1947.

31. Kim CH, et al. (2000) Repressor activity of Headless/Tcf3 is essential for vertebrate head formation. *Nature* 407(6806):913–916.

32. Houston DW, et al. (2002) Repression of organizer genes in dorsal and ventral Xenopus cells mediated by maternal XTcf3. *Development* 129(17):4015–4025.

33. Wu CI, et al. (2012) Function of Wnt/β-catenin in counteracting Tcf3 repression through the Tcf3-β-catenin interaction. *Development* 139(12):2118–2129.

34. Douglas KR, et al. (2001) Identification of members of the Wnt signaling pathway in the embryonic pituitary gland. *Mamm Genome* 12(11):843–851.

35. Wang X, Lee JE, Dorsky RI (2009) Identification of Wnt-responsive cells in the zebrafish hypothalamus. *Zebrafish* 6(1):49–58.

36. Wilson SW, Houart C (2004) Early steps in the development of the forebrain. *Dev Cell* 6(2):167–181.

37. Olson LE, et al. (2006) Homeodomain-mediated beta-catenin-dependent switching events dictate cell-lineage determination. *Cell* 125(3):593–605.

38. Cha KB, et al. (2004) WNT5A signaling affects pituitary gland shape. *Mech Dev* 121(2):183–194.

39. Potok MA, et al. (2008) WNT signaling affects gene expression in the ventral diencephalon and pituitary gland growth. *Dev Dyn* 237(4):1006–1020.

40. Brinkmeier ML, et al. (2003) TCF and Groucho-related genes influence pituitary growth and development. *Mol Endocrinol* 17(11):2152–2161.

41. Brinkmeier ML, Potok MA, Davis SW, Camper SA (2007) TCF4 deficiency expands ventral diencephalon signaling and increases induction of pituitary progenitors. *Dev Biol* 311(2):396–407.

42. Yi F, et al. (2011) Opposing effects of Tcf3 and Tcf1 control Wnt stimulation of embryonic stem cell self-renewal. *Nat Cell Biol* 13(7):762–770.

43. Yi F, Pereira L, Merrill BJ (2008) Tcf3 functions as a steady-state limiter of transcriptional programs of mouse embryonic stem cell self-renewal. *Stem Cells* 26(8):1951–1960.

44. Nguyen H, et al. (2009) Tcf3 and Tcf4 are essential for long-term homeostasis of skin epithelia. *Nat Genet* 41(10):1068–1075.

45. Merrill BJ, et al. (2004) Tcf3: A transcriptional regulator of axis induction in the early embryo. *Development* 131(2):263–274.

46. Hoffman JA, Wu CI, Merrill BJ (2013) Tcf7l1 prepares epiblast cells in the gastrulating mouse embryo for lineage specification. *Development* 140(8):1665–1675.

47. Andoniadou CL, et al. (2011) HESX1- and TCF3-mediated repression of Wnt/β-catenin targets is required for normal development of the anterior forebrain. *Development* 138(22):4931–4942.

48. Andoniadou CL, Martinez-Barbera JP (2013) Developmental mechanisms directing early anterior forebrain specification in vertebrates. *Cell Mol Life Sci* 70(20):3739–3752.

49. Andoniadou CL, et al. (2007) Lack of the murine homeobox gene Hesx1 leads to a posterior transformation of the anterior forebrain. *Development* 134(8):1499–1508.

50. Gaston-Massuet C, et al. (2011) Increased Wingless (Wnt) signaling in pituitary progenitor/stem cells gives rise to pituitary tumors in mice and humans. *Proc Natl Acad Sci USA* 108(28):11482–11487.

51. Jayakody SA, et al. (2012) SOX2 regulates the hypothalamic-pituitary axis at multiple levels. *J Clin Invest* 122(10):3635–3646.

52. Meyers EN, Lewandoski M, Martin GR (1998) An Fgf8 mutant allelic series generated by Cre- and Flp-mediated recombination. *Nat Genet* 18(2):136–141.

53. Gaston-Massuet C, et al. (2008) Genetic interaction between the homeobox transcription factors HESX1 and SIX3 is required for normal pituitary development. *Dev Biol* 324(2):322–333.

54. Sajedi E, et al. (2008) Analysis of mouse models carrying the I26T and R160C substitutions in the transcriptional repressor HESX1 as models for septo-optic dysplasia and hypopituitarism. *Dis Model Mech* 1(4-5):241–254.

55. Trowe MO, et al. (2013) Inhibition of Sox2-dependent activation of Shh in the ventral diencephalon by Tbx3 is required for formation of the neurohypophysis. *Development* 140(11):2299–2309.

56. Gribble SL, Kim HS, Bonner J, Wang X, Dorsky RI (2009) Tcf3 inhibits spinal cord neurogenesis by regulating sox4a expression. *Development* 136(5):781–789.

57. Kimmel CB, Ballard WW, Kimmel SR, Ullmann B, Schilling TF (1995) Stages of embryonic development of the zebrafish. *Dev Dyn* 203(3):253–310.

58. Treier M, et al. (2001) Hedgehog signaling is required for pituitary gland development. *Development* 128(3):377–386.

59. Zhao L, et al. (2012) Disruption of SoxB1-dependent Sonic hedgehog expression in the hypothalamus causes septo-optic dysplasia. *Dev Cell* 22(3):585–596.

60. McCabe MJ, Alatzoglou KS, Dattani MT (2011) Septo-optic dysplasia and other midline defects: The role of transcription factors: HESX1 and beyond. *Best Pract Res Clin Endocrinol Metab* 25(1):115–124.

61. Dattani MT, et al. (1998) Mutations in the homeobox gene HESX1/Hesx1 associated with septo-optic dysplasia in human and mouse. *Nat Genet* 19(2):125–133.

62. Sykiotis GP, et al. (2010) Oligogenic basis of isolated gonadotropin-releasing hormone deficiency. *Proc Natl Acad Sci USA* 107(34):15140–15144.

63. Gregory LC, et al. (2014) The role of the sonic hedgehog signalling pathway in patients with midline defects and congenital hypopituitarism. *Clin Endocrinol (Oxf)* 82(5):728–738.

64. Pfaeffle RW, et al. (2008) Three novel missense mutations within the LHX4 gene are associated with variable pituitary hormone deficiencies. *J Clin Endocrinol Metab* 93(3):1062–1071.

65. Hikasa H, et al. (2010) Regulation of TCF3 by Wnt-dependent phosphorylation during vertebrate axis specification. *Dev Cell* 19(4):521–532.

66. Hikasa H, Sokol SY (2011) Phosphorylation of TCF proteins by homeodomain-interacting protein kinase 2. *J Biol Chem* 286(14):12093–12100.

Gaston-Massuet et al.

DEVELOPMENTAL BIOLOGY

www.manaraa.com